

Transient Response Analysis of a MESFET Amplifier Illuminated by an Intentional EMI Source

Qi-Feng Liu¹, Jing-Wei Liu², Chong-Hua Fang¹

¹Science and Technology on EMC Laboratory, Wuhan, China, emclqf@126.com

²Wuhan Wuda Jucheng Strengthening Industrial Co. Ltd, Wuhan, China

Abstract—Unintentional as well as intentional electromagnetic interference can cause improper functionality of microwave circuits or systems. In this paper, our attention is focused on transient response characterization of microwave MESFET amplifiers, which are used widely in the integration of communication circuits and systems, under the impact of an intentional electromagnetic interference(IEMI) source but with different waveforms, respectively. The mathematical treatment is based on two-port lumped networks FDTD method. Parametric studies are carried out to shows effects of the EMI waveforms, its magnitudes on the transient coupled voltages on the input-output of the microwave MESFET amplifiers, with sufficient information obtained for understanding the interaction between the IEMI source and the microwave MESFET amplifier.

Key Words- Electromagnetic pulses (EMP), microwave amplifier, MESFET device, two-port lumped-network, FDTD.

I. INTRODUCTION

Intentional electromagnetic interference (IEMI) refers to “intentional malicious generation of electromagnetic energy introducing noise or signals into electrical and electronic systems, thus disrupting, confusing, or damaging these systems for terrorist or criminal purposes”[1]. Such an IEMI can be generated by a high-power microwave source, such as a pulse antenna. On the other hand, it is known that the trend of microwave circuits is being moved towards highly hybrid integrated system, such as monolithic microwave integrated circuits (MMIC), *etc.* Physically, a microwave amplifier with active devices can be easily disturbed by a EMI source, such as an ultra-wideband EMP.

Generally speaking, there are two major approaches for incorporating passive and active lumped devices into finite-difference time-domain (FDTD) method to analyze the hybrid microwave circuit [2]. One approach is to use the S-parameters to represent the devices [3] and the other is to use an equivalent SPICE model to account for the devices [4]. In this paper, our attention is focused on using the two-port lumped-network FDTD (TP-LN FDTD) method to investigate

transient responses of a microwave MESFET amplifier illuminated by an external EMI.

II. FROMULATION

To incorporate the two-port lumped network (TP-LN) into the FDTD method, two electrical nodes are used to interface the FDTD mesh with two-port lumped networks. The two symmetric electrical E_{x1} and E_{x2} are used to interface with the lumped networks, as shown in Fig. 1(a), and the Ampere’s equation, at nodes E_{x1} and E_{x2} , is then complemented by adding current density term J_{x1} and J_{x2} to take the lumped networks into account [4], respectively. This term is discretized by using a time average, so we can obtain the following equations:

$$E_{x1}^{n+1} = E_{x1}^n + \frac{\Delta t}{\epsilon} \left[\nabla \times \vec{H} \right]_{x1}^{n+\frac{1}{2}} - \frac{\Delta t}{2\epsilon} (J_{x1}^{n+1} + J_{x1}^n) \quad (1)$$

$$E_{x2}^{n+1} = E_{x2}^n + \frac{\Delta t}{\epsilon} \left[\nabla \times \vec{H} \right]_{x2}^{n+\frac{1}{2}} - \frac{\Delta t}{2\epsilon} (J_{x2}^{n+1} + J_{x2}^n) \quad (2)$$

The two-port networks are defined in terms of its admittance matrix in the Laplace domain as follows:

$$\begin{bmatrix} I_1(s) \\ I_2(s) \end{bmatrix} = \begin{bmatrix} Y_{11}(s) & Y_{12}(s) \\ Y_{21}(s) & Y_{22}(s) \end{bmatrix} \begin{bmatrix} V_1(s) \\ V_2(s) \end{bmatrix} \quad (3)$$

where I_p and V_p , $p=1,2$ are the port terminal current and voltage, respectively.

In the Laplace domain, the V-I relation of a two-port lumped-network can be expressed as

$$I_p(s) = \sum_{q=1,2} Y_{pq}(s) \cdot V_q(s) \quad (4)$$

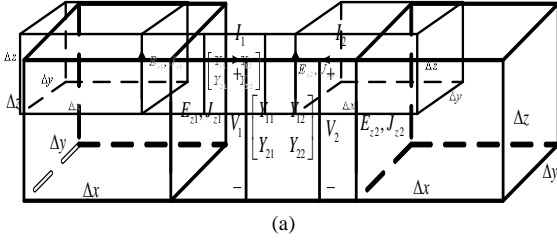
where the admittance $Y_{pq}(s)$ is a rational function for one-port and a matrix consisting of rational functions for multi-port cases, respectively. Therefore, we have

$$Y_{pq}(s) = \sum_{m=0}^{M_{pq}} a_m^{(p,q)} s^m / \sum_{n=0}^{N_{pq}} b_n^{(p,q)} s^n \quad (5)$$

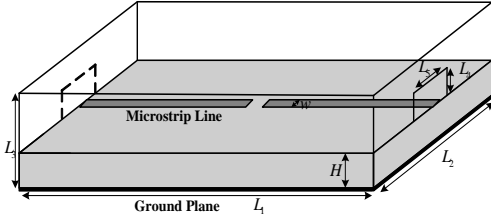
where $a_m^{(p,q)}$ and $b_n^{(p,q)}$ are real-valued coefficients, M_{pq} and N_{pq} are the order numbers of the model, respectively. We can change the $Y(s)$ into the Z -domain using the bilinear transform [5]. In the Z -domain, (5) is turned into

$$Y_{pq}(Z^{-1}) = \sum_{m=0}^{M_{pq}} c_m^{(p,q)} Z^{-m} / \sum_{n=0}^{N_{pq}} d_n^{(p,q)} Z^{-n} \quad (6)$$

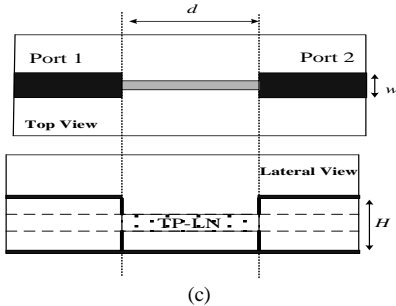
where the coefficients $p_m^{(p,q)}$ and $q_n^{(p,q)}$ are obtained from $a_m^{(p,q)}$ and $b_n^{(p,q)}$, and this discretization procedure preserves the second-order accuracy of the conventional FDTD.



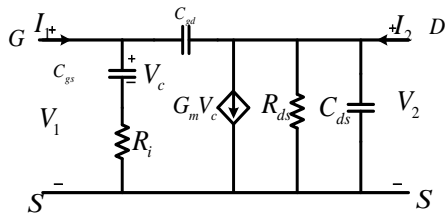
(a)



(b)



(c)



(d)

Fig. 1. The configuration of a MEFET microwave circuit. (a) The TP-LN connected to two FDTD cells, (b) three-dimensional structure, (c) Top and lateral view of the hybrid circuit, and (d) the equivalent circuit for MEFET.

To transfer (4) into the Z -domain, we have

$$I_{pq}^{n+1} + \sum_{m=1}^{M_{pq}} d_m^{(p,q)} I_{pq}^{n-m+1} = \sum_{m=0}^{M_{pq}} c_m^{(p,q)} V_q^{n-m+1} \quad (7)$$

where $V_q^n \approx E_{xq}^n \Delta x$ and $I_p^{n+\frac{1}{2}} \approx J_{xp}^{n+\frac{1}{2}} \Delta y \Delta z$, then we can obtain from above equations that

$$\begin{bmatrix} \varepsilon E_{x1}^{n+1} \\ \varepsilon E_{x2}^{n+1} \end{bmatrix} = \begin{bmatrix} 1 + \frac{\Delta t}{2} \bar{C}_0^{(1,1)} & \frac{\Delta t}{2} \bar{C}_0^{(1,2)} \\ \frac{\Delta t}{2} \bar{C}_0^{(2,1)} & 1 + \frac{\Delta t}{2} \bar{C}_0^{(2,2)} \end{bmatrix}^{-1} \begin{bmatrix} T_{x1}^n \\ T_{x2}^n \end{bmatrix} \quad (8a)$$

$$T_{xp}^n = \varepsilon E_{xp}^n + \Delta t (\nabla \times \bar{H})_{xp}^{n+1/2} - \frac{\Delta t}{2} (J_{xp1}^n + A_{xp1}^n + J_{xp2}^n + A_{xp2}^n) \quad (8b)$$

$$A_{xpq}^n = - \sum_{m=M_{pq}}^{M_{pq}} d_m^{(p,q)} J_{x,pq}^{n-m+1} + \sum_{k=N_{pq}}^{N_{pq}} \bar{C}_m^{(p,q)} \varepsilon E_{xp}^{n-k+1} \quad (8c)$$

$$J_{x,pq}^n = - \sum_{m=1}^{M_{pq}} d_m^{(p,q)} J_{x,pq}^{n-m+1} + \sum_{k=0}^{N_{pq}} \bar{C}_m^{(p,q)} \varepsilon E_{xp}^{n-k+1} \quad (8d)$$

Therefore, this equation allows a two-port lumped-network to be incorporated into the FDTD, but still preserving the explicit nature of the Yee's scheme.

III. NUMERICAL RESULTS AND DISCUSSIONS

We consider the equivalent circuit of the linear model of a general MESFET microwave amplifier [4]. The MESFET device is placed at the microstrip gap, as shown in Figs. 1(b) and 1(c), respectively. The scattering parameters of the hybrid circuits are captured by the TPLN-FDTD algorithm. It spans several FDTD cells, which corresponds to the length of the microstrip gap. The four ideal wire of single cell are used to connect the MESFET device to the strips and to the ground. The microstrip substrate has dielectric constant $\varepsilon_r = 2.17$ and a thickness $H = 0.254 \text{ mm}$. The line width is $w = 0.79 \text{ mm}$, which corresponds to an impedance of approximately 50Ω . The microwave amplifier is illuminated by an external EMP, and it is described by a triple-exponential function as follows:

$$E^{(inc)} = E_0 \times \sum_{p=1}^3 a_i^p e^{-\left(\frac{r-t_i^p}{z_i^p}\right)^2} \quad (9)$$

To check the accuracy of our two-port lumped-network FDTD code, we at first to calculate the S-parameters of the microwave MESFET amplifier, with no external EMI source implemented. The S-parameters are obtained using the Fourier transform at the end of FDTD iteration. The input and output voltages at points 1 and 2 are shown in Fig. 2, respectively. Fig. 3 shows the simulated S-parameters of the microwave amplifier, as compared with the ADS results given in [4]. It is obvious that excellent agreements are obtained between them.

Then, we pay our attention to the transient response of the microwave MESFET amplifier, illuminated by an external high-power EMP. The incident EMP direction is set to be $\varphi = 135^\circ$ and $\theta = 90^\circ$, with a polarization angle of 90° assumed. In our simulation, the output and input ports are terminated by a 50Ω matched load, respectively, when the

amplifier is illuminated by an external EMI source. The induced voltages at the input/output ports of Fig.1 (c) and the two terminals of the MESFET device in Fig.1(d) are plotted in Fig. 4 for $E_0 = 58kV/m$. It is found that the external high-power wideband EMP can induce as high as 11.09 V and 2.1 V voltages at the output/input ports, and even as high as 16.98V and 1.48V at the two device terminals, respectively.

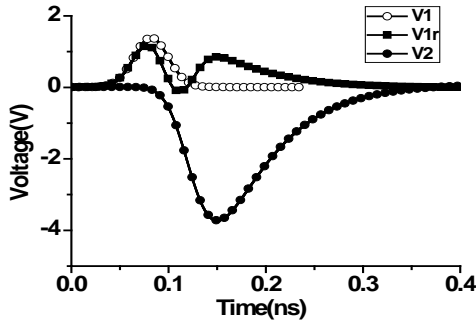


Fig. 2. The reflected and total voltage at input/output ports, respectively.

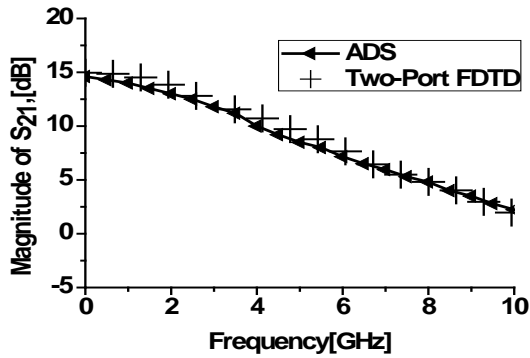
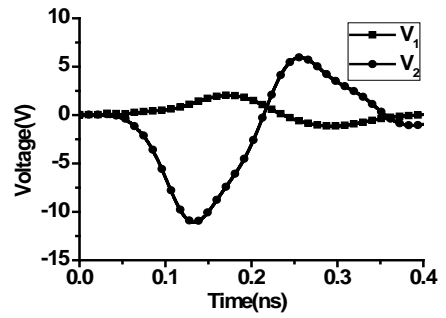


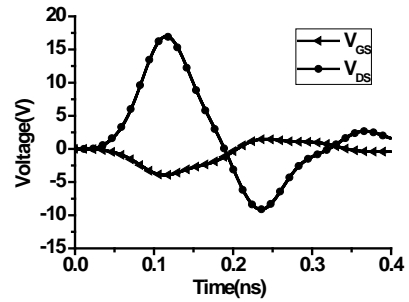
Fig. 3. Comparisons of S-parameters in the TPLN-FDTD and ADS.

We now change the magnitude E_0 of the incident intentional EMI source, and set it to be $2.9 kV/m$, and $5.8 kV/m$, respectively. For practical case, the amplifier will be shielded by a metallic enclosure. Under such circumstances, the inner input EMI signal magnitude will be much smaller than that of the external source.

In Fig. 5, it is shown that as the magnitude of the incident EMP decreases, low voltage signals are induced at two output ports, as compared with those in Fig. 4(a), respectively. Therefore, it is important to design the some packaging enclosure to further suppress the EMI signal impact on the amplifier.

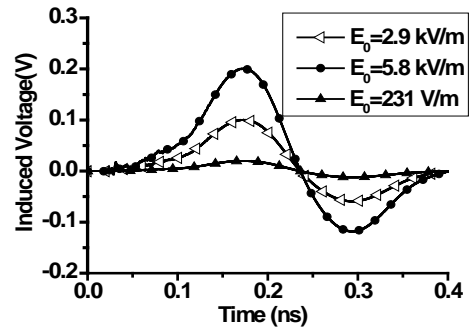


(a)

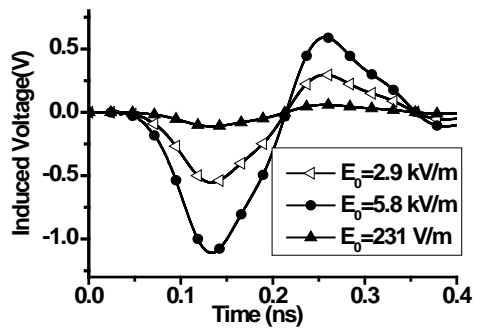


(b)

Fig. 4. (a)The induced voltages at the input/output ports of the amplifier, respectively; and (b) the induced voltages at the device terminals.



(a)



(b)

Fig. 5. The induced voltages of the amplifier for different magnitudes of the incident EMP recorded at (a) at input port (b) at output port.

IV. CONCLUSION

The FDTD method is implemented to characterize EMI effects on the microwave MESFET amplifier caused by an external IEMI source. According to our simulation, the effects of different geometrical and physical parameters of the devices as well as the waveform parameters of the IEMI source on the interfere responses at both input and output ports can be predicted. Of course, certain protection method can be further implemented so as to suppress the IEMI impact on the wideband communication circuits and systems.

REFERENCES

- [1] W. A. Radasky, C. E. Baum, and M. W. Wik, "Introduction to the special issue on high-power electromagnetics (HPEM) and intentional electromagnetic interference (IEMI)," *IEEE Trans. Electromagn. Compat.*, vol. 46, no. 3, pp. 314-321, 2004.
- [2] C. C. Wang, C. W. Kuo, "An efficient scheme for processing arbitrary lumped multiport devices in the finite-difference time-domain method," *IEEE Trans. Microwave Theory Tech.*, vol. 55, no.3, pp. 958-965, May 2007.
- [3] X.Ye and J. L. Drewniak, "Incorporating two-port networks with S-parameters into FDTD," *IEEE Microw. Wireless Compon. Lett.*, vol. 11,no. 2, pp. 77-79, Feb. 2001.
- [4] O. Gonzalez, J. A. Pereda, A. Herrera, and A. Vegas, "An extension of the lumped-network FDTD method to linear two-port lumped circuits," *IEEE Trans. Microw. Theory Tech.*, vol. 54, no. 7, pp. 3045-3051, Jul. 2006.
- [5] X. T. Dong, W. Y. Yin, and Y. B. Gan, "Perfectly matched layer implementation using bilinear transform for microwave device applications," *IEEE Trans. Microw. Theory Tech.*, vol. 53, no. 10, pp. 3098-3105, Oct. 2005.